

The effect of local lattice distortion on physical properties of hexagonal rubidium tungsten bronze $\text{Rb}_{0.23}\text{WO}_y$

This content has been downloaded from IOPscience. Please scroll down to see the full text.

2009 J. Phys.: Conf. Ser. 150 052141

(<http://iopscience.iop.org/1742-6596/150/5/052141>)

View [the table of contents for this issue](#), or go to the [journal homepage](#) for more

Download details:

IP Address: 163.13.36.187

This content was downloaded on 14/04/2015 at 05:47

Please note that [terms and conditions apply](#).

The effect of local lattice distortion on physical properties of hexagonal rubidium tungsten bronze $\text{Rb}_{0.23}\text{WO}_y$

D.C. Ling^{1*}, Y.C. Shao¹, J.W. Chiou², W.F. Pong¹, S.H. Wu³, Y.Y. Chen³, and F.Z. Chien¹

¹Department of Physics, Tamkang University, Tamsui 25137, Taiwan

²Department of Applied Physics, National University of Kaohsiung, Nanzih 81148, Taiwan

³Institute of Physics, Academia Sinica, Taipei 11529, Taiwan

E-mail: dcling@mail.tku.edu.tw

Abstract. Superconducting transition temperature T_c and normal-state resistivity as a function of oxygen content for hexagonal tungsten bronze $\text{Rb}_{0.23}\text{WO}_y$ with $2.90 < y < 3.05$ were obtained from transport measurements. It is remarkably interesting that T_c enhances about 50% and room-temperature resistivity increases about three orders of magnitude as oxygen content varies from 2.90 to 3.05. The low-temperature specific heat data indicate that the Einstein-like mode associated with Rb vibration has a dimensionality crossover from 3D to quasi-2D as oxygen content increases from 2.90 to 3.05. $W L_3$ -edge x-ray absorption spectra further show that W-O bond intensity gradually weakens as oxygen content increases, indicative of more oxygen disorder present in the oxygen-rich samples. The observed results strongly suggest that the local lattice distortion induced by oxygen disorder not only modulates Rb vibration, possibly coupled to electron-phonon interaction responsible for superconductivity, and also reduces the charge transfer between O $2p$ and W $5d$ orbital in the vicinity of $y=3.00$. This scenario can possibly account for significant increases of T_c and normal-state resistivity of $\text{Rb}_{0.23}\text{WO}_y$ as oxygen content slightly changes from 2.90 to 3.05.

1. Introduction

Tungsten bronzes M_xWO_3 ($M =$ alkali atoms) have attracted a great deal of interest for years because of their interesting structural and electronic properties as well as the potential applications in electrochromic devices and solid electrolytes [1]. It is well known that tungsten bronzes can crystallize a variety of structures including tetragonal tungsten bronze (TTB), hexagonal tungsten bronze (HTB), and intergrowth tungsten bronze (ITB). Among them, the HTB has been demonstrated to be more favorable to superconductivity than other structures [2-3]. The building block of the HTBs is corner-linked distorted WO_6 octahedra and hexagonal tunnels formed by the linkage along the c -axis where alkali atoms are accommodated. The structure of HTB M_xWO_3 is stabilized by larger alkali atoms intercalation such as K, Rb, and Cs with $0.19 \leq x \leq 0.33$. R.K. Stanley *et al.* showed that Rb_xWO_3 has the highest superconducting transition temperature T_c among the HTBs [4]. More recently, R. Brusetti *et al.* reported that T_c monotonically decreases from 5 K to 0.2 K in the range of $0.19 < x < 0.25$ and then increases to 3 K in the range of $0.25 < x < 0.33$ for HTB Rb_xWO_3 [5]. It has been suggested that

* To whom any correspondence should be addressed.

the structural instability induced by the ordering of rubidium vacancies below 240 K might be responsible for the lowest T_c of 0.2 K observed near $x = 0.25$ [5]. Nevertheless, up to date, no consensus is emerged about the origin of the anomalous $T_c(x)$ dependence.

To shed light on how the superconducting properties of the HTBs are modulated by doping, an alternative approach, by varying oxygen content instead of rubidium content, was taken. A series of single-phased $\text{Rb}_{0.23}\text{WO}_y$ compounds with $2.90 < y < 3.05$ were synthesized. The reason for making samples with rubidium content $x = 0.23$ is that inevitable impurity phases arising from intergrowth tungsten bronze for $0.19 < x < 0.215$ are commonly observed and a poorly crystalline phase is formed for $0.27 < x < 0.33$ [6]. The extensive investigations on transport properties, low-temperature specific heat (LTSH) and x-ray absorption spectra suggest that oxygen content has a significant influence on the nature of physical properties of $\text{Rb}_{0.23}\text{WO}_y$.

2. Experimental

Samples investigated were synthesized by the solid-state reaction method. Purity of the samples was characterized by powder x-ray diffraction (XRD) with Cu K_α radiation. Detailed synthesis conditions and XRD results have been reported elsewhere [6]. Transport properties were performed by PPMS. Specific heat measurements were made by a thermal-relaxation microcalorimeter. W L_3 -edge x-ray absorption spectra were obtained at the National Synchrotron Radiation Research Center, Hsinchu, Taiwan.

3. Results and Discussion

As shown in Fig. 1(a), T_c is around 3 K in the low oxygen content regime ($2.90 < y < 2.95$) and is then suppressed below 2 K for $2.95 < y < 3.00$ as plotted in open circles. More interestingly, T_c enhances significantly up to ~ 4.5 K in the high oxygen content regime ($3.00 < y < 3.05$). The oxygen content dependence of the $\rho_{300\text{K}}$ for $\text{Rb}_{0.23}\text{WO}_y$ is displayed in Fig. 1(b). It appears that the normal-state resistivity of the samples with $y > 3.00$ is about three orders of magnitude larger than that of those with $y < 3.00$. Furthermore, metallic behavior with $d\rho/dT > 0$ is observed in the normal-state of $\text{Rb}_{0.23}\text{WO}_y$ with $y < 3.00$, whereas a distinctly different feature with $d\rho/dT < 0$ is observed in the normal-state of $\text{Rb}_{0.23}\text{WO}_y$ with $y > 3.0$. The two representative $\rho(T)$ curves for $\text{Rb}_{0.23}\text{WO}_{2.90}$ and $\text{Rb}_{0.23}\text{WO}_{3.04}$ are plotted in Figs. 1(c) and 1(d), respectively for comparison.

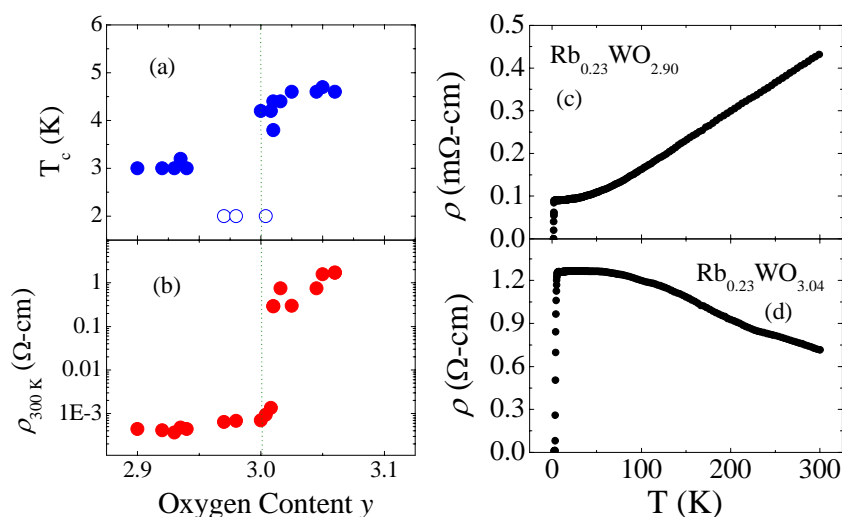


Figure 1. (a) $T_c(y)$ for $\text{Rb}_{0.23}\text{WO}_y$. The open circles in the vicinity of $y \sim 3.00$ means that no superconductivity was observed down to 2 K. (b) $\rho_{300\text{K}}(y)$ for $\text{Rb}_{0.23}\text{WO}_y$. (c) and (d) are representative $\rho(T)$ curves for $y = 2.90$ and 3.04 samples, respectively.

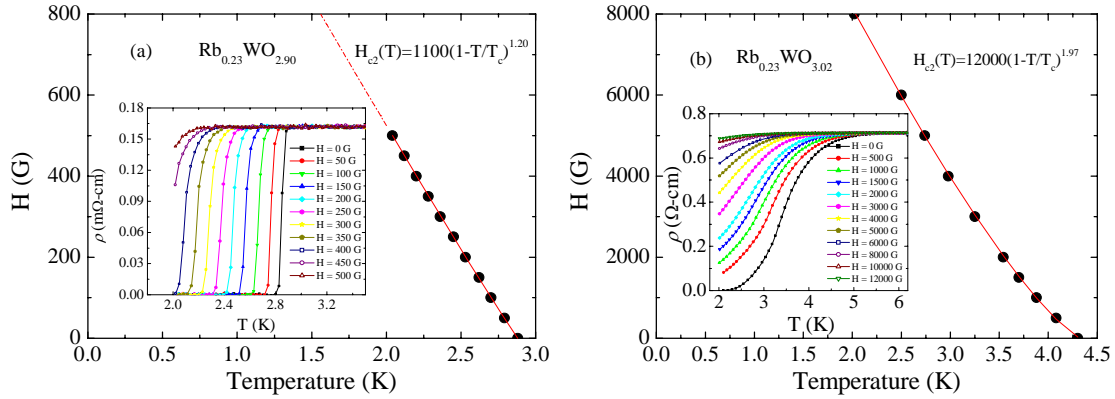


Figure 2. (a) Magnetic phase diagram $H_{c2}(T)$ for $\text{Rb}_{0.23}\text{WO}_{2.90}$. (b) $H_{c2}(T)$ for $\text{Rb}_{0.23}\text{WO}_{3.02}$. The dashed line corresponds to the phenomenological relation $H_{c2}(T) = H_{c2}(0)[1-(T/T_c)^2]^\alpha$. The insets of (a) and (b) display $\rho(T)$ at different fields for $\text{Rb}_{0.23}\text{WO}_{2.90}$ and $\text{Rb}_{0.23}\text{WO}_{3.02}$, respectively.

$\rho(T)$ at different fields for $\text{Rb}_{0.23}\text{WO}_{2.90}$ and $\text{Rb}_{0.23}\text{WO}_{3.02}$ are present in the insets of Figs. 2(a) and 2(b), respectively. It is clear that oxygen-deficient sample $\text{Rb}_{0.23}\text{WO}_{2.90}$ has a sharper superconducting transition width comparing with oxygen-rich sample $\text{Rb}_{0.23}\text{WO}_{3.02}$. It should be noted that the sharper transition width accompanied by a lower T_c is consistently observed in Rb_xWO_y with $y < 3.0$ and $0.19 < x < 0.27$ [6]. The $H_{c2}(T)$ phase diagram illustrated in Figs. 2(a) and 2(b) are extracted from 10% drop of normal-state resistivity at various magnetic fields. The dashed line is the phenomenological relation $H_{c2}(T) = H_{c2}(0)[1-(T/T_c)^2]^\alpha$ with the fitted $H_{c2}(0)$ about 1100 G for $\text{Rb}_{0.23}\text{WO}_{2.90}$ and 12000 G for $\text{Rb}_{0.23}\text{WO}_{3.02}$, respectively. Also, the exponent α for $\text{Rb}_{0.23}\text{WO}_{2.90}$ is 1.20 close to the value of two-fluid model and for $\text{Rb}_{0.23}\text{WO}_{3.02}$ is 1.97 similar to observed values in high- T_c cuprates.

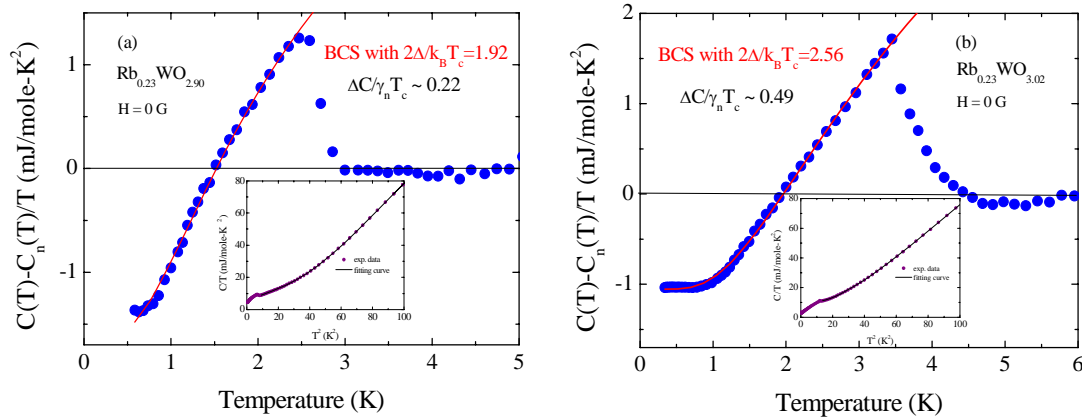


Figure 3. (a) and (b) are zero-field $[C(T)-C_n(T)]/T$ versus T plots for $\text{Rb}_{0.23}\text{WO}_{2.90}$ and $\text{Rb}_{0.23}\text{WO}_{3.02}$. The insets are zero-field $C(T)/T$ versus T^2 plots for $\text{Rb}_{0.23}\text{WO}_{2.90}$ and $\text{Rb}_{0.23}\text{WO}_{3.02}$.

The zero-field $C(T)/T$ versus T^2 plots for $\text{Rb}_{0.23}\text{WO}_{2.90}$ and $\text{Rb}_{0.23}\text{WO}_{3.02}$ are shown in the insets of Fig. 3(a) and 3(b). The normal-state LTSH data can be best fitted to $C_n(T) = \gamma_n T + \beta T^3 + 0.23nN_A k_B (T_E/T)^2 \exp(-T_E/T)$, where T_E is the Einstein temperature, $0.23nN_A k_B (T_E/T)^2 \exp(-T_E/T)$ is the expression for Einstein mode associated with n -dimensional Rb vibration at $T \ll T_E$. The fitted parameters exhibit strong oxygen-dependent with $\gamma_n = 4.705 \text{ mJ/mol}\cdot\text{K}^2$, $\beta = 0.345 \text{ mJ/mol}\cdot\text{K}^4$ and

$T_E = 64.1$ K for $\text{Rb}_{0.23}\text{WO}_{2.90}$ and $\gamma_n = 3.775$ mJ/mol-K², $\beta = 0.471$ mJ/mol-K⁴ and $T_E = 62.9$ K for $\text{Rb}_{0.23}\text{WO}_{3.02}$. More importantly, the fitted value of n is 2.98 and 2.21 for samples with $y = 2.90$ and 3.02, respectively. It indicates that the Einstein mode associated with Rb vibration possibly has a dimensionality crossover from 3D to quasi-2D as y increases. In addition, Figs. 3(a) and 3(b) show that the estimated $2\Delta/k_B T_c$ is ~ 1.92 and 2.56 for samples with $y = 2.90$ and 3.02, $[C(T) - C_n(T)]/\gamma_n T_c$ is ~ 0.22 for $\text{Rb}_{0.23}\text{WO}_{2.90}$ and 0.49 for $\text{Rb}_{0.23}\text{WO}_{3.02}$, respectively. It should be noted that both the $2\Delta/k_B T_c$ and $[C(T) - C_n(T)]/\gamma_n T_c$ are much smaller than the values predicated by the BCS theory in the weak-coupling limit. More investigations are needed to have better understanding of the intriguing results.

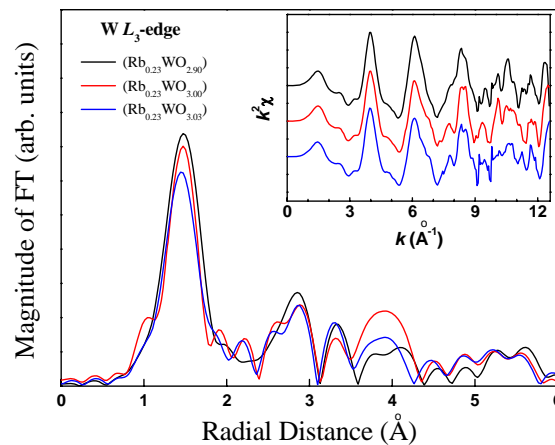


Figure 4. FT of W L_3 -edge EXAFS spectra for $\text{Rb}_{0.23}\text{WO}_y$. The inset plots the corresponding $k^3\chi$ data.

Fourier transform (FT) of W L_3 -edge extended x-ray absorption fine structure (EXAFS) spectra is displayed in Fig. 4. It reveals that W-O bond intensity gradually weakens as oxygen content increases, indicative of more oxygen disorder present, inducing a local lattice distortion of WO_6 octahedra with a contraction along the c -axis and an elongation in the a -axis [8], in the oxygen-rich samples. As a result, it profoundly weakens $W5d\text{-O}2p$ hybridizations and leads to a larger value of normal-state resistivity for samples with higher oxygen content.

In summary, the observed results strongly suggest that the local lattice distortion induced by oxygen disorder not only modulates Rb vibration, possibly coupled to electron-phonon interaction responsible for superconductivity, and also reduces the charge transfer between O $2p$ and W $5d$ orbital of $\text{Rb}_{0.23}\text{WO}_y$ in the vicinity of $y = 3.00$. This scenario can possibly account for significant increases of T_c and normal-state resistivity of $\text{Rb}_{0.23}\text{WO}_y$ as oxygen content slightly changes from 2.90 to 3.05.

Acknowledgements

This work was financially supported by the National Science Council of ROC under grant No. NSC 96-2212-M-032-008-MY3.

References

- [1] Raub C J, Sweedler A R, Broadston S and Matthias B T 1964 *Phys. Rev. Lett.* **13** 746
- [2] Krause H B, Vincent R and Steeds J W 1988 *Solid State Commun.* **68** 937
- [3] Sato M, Grier B H, Shirane G and Fujishita H 1982 *Phys. Rev. B* **25** 501
- [4] Stanley R K, Morris R C and Moulton W G 1979 *Phys. Rev. B* **20** 1903
- [5] Brusetti R, Haen P and Marcus J 2002 *Phys. Rev. B* **65** 144528
- [6] Ting L C, Hsieh H H, Kang H H, Ling D C, Liu H L, Pong W F, Chien F Z and Hor P H 2007 *J. Supercond. Novel Mag.* **20** 249
- [7] Ting L C *et al.*, 2007 *Chin. J. Phys.* **45** 237
- [8] Magneli A 1953 *Acta Chem. Scand.* **7** 315; Ting L C *et al.*, 2002 *J. Supercond.* **15** 675